2011 International Workshop on ADC Modelling, Testing and Data Converter Analysis and Design and IEEE 2011 ADC Forum
June 30 - July 1, 2011. Orvieto, Italy.

Digital background calibration of subsampling time-interleaved ADCs

Francesco Centurelli, Pietro Monsurrò, Alessandro Trifiletti

Dipartimento di Ingegneria dell'Informazione, Elettronica e Telecomunicazioni
Università di Roma La Sapienza
Via Eudossiana, 18 – 00184 Roma, ITALY
centurelli@die.uniroma1.it, monsurro@die.uniroma1.it, trifiletti@die.uniroma1.it

***Abstract*-**A technique for the digital background calibration of subsampling time-interleaved analog-to-digital converters is proposed. The technique corrects the errors due to gain, offset and timing mismatches among the time-interleaved channels by estimating and nulling the errors with respect to a reference channel through least mean squares loops. Wideband undersampled differentiator filters are exploited thus enabling digital background calibration of timing skews even with wideband input signals outside the first Nyquist band.

I. Introduction

Software-defined radio (SDR) receivers benefit from digitizing RF analog signals early-on in the receiver path, to exploit the advantages of digital processing; the analog-to-digital converter (ADC) also acts as frequency downconverter, by undersampling the input signal to baseband. This requires a very wide analog bandwidth, and a sampling frequency that is at least twice the bandwidth of the signal. Time-interleaved (TI) ADCs are a possible solution to achieve high accuracy and high sampling frequency using several slow but accurate ADCs in parallel [1]-[2]. However, the performance of TI-ADCs is limited by offset, gain and timing mismatches among the ADC channels, that reduce the achievable linearity [3], limiting the possibilities of employing this technique. Errors that are tolerable on a single-channel ADC can give rise to distortion when in a time-interleaved configuration.

Several solutions have been presented in the literature for the background calibration of TI-ADCs. The most efficient calibration algorithms operate in the digital domain and are based on least mean squares (LMS) loops that use a reference ADC (or the split-ADC configuration [4]). The technique used to estimate and calibrate the timing mismatches sets a limit on the fraction of the Nyquist bandwidth that can be effectively exploited by the TI-ADC. McNeill et al. in [4] approximate the timing delay with a first-order Taylor expansion, and calculate the derivative with a three-tap FIR filter. Oshima et al. in [5] use a higher-order FIR approximation to estimate the derivative, and correct also for the second-order Taylor expansion term (dependent on the second-order derivative). Most of the calibration techniques in the literature are not directly applicable to undersampling time-interleaved converters; calibration of undersampling TI-ADCs is treated in [6], but under the assumption of narrowband signals.

This paper builds on [4] and [5] to obtain the calibration of TI-ADCs in a wider fraction of the Nyquist band, also for signals in the successive Nyquist bands, by developing wideband differentiator filters for undersampled signals. The paper is structured as follows: Section II introduces the architecture and the design issues of TI-ADCs and describes the proposed calibration algorithm, Section III explores the issue of the design of filters to compute the derivative of the input signal, and Section IV is dedicated to the computation of the time derivative of undersampled input signals. Simulation results are presented in Section V.

II. Time-interleaved converters and calibration algorithm

Fig. 1 (neglect ADC3) shows the architecture of a two-channel TI-ADC. The input signal $V_{IN}(t)$ is applied to the two converters in parallel, each operating at a sampling frequency of $f_S/2$. The two channels have to be clocked with a delay of $1/f_S$ to ensure uniform sampling, thus allowing to double up to f_S the overall sampling frequency of the converter, since odd and even samples are separately converted by the two constituent ADCs.

Generalization of the architecture for a higher number of channels is straightforward, since M converters working at f_S/M sampling frequency, each clocked with a $1/f_S$ delay with respect to the following one, suffice to convert a signal at an overall sampling frequency of f_S. Slow but accurate ADCs can thus be interleaved to obtain a faster ADC, for a total power consumption which is roughly equal to M times that of a single converter, plus some overhead due to the generation of the lower-frequency clock signals and the recombination of the digital

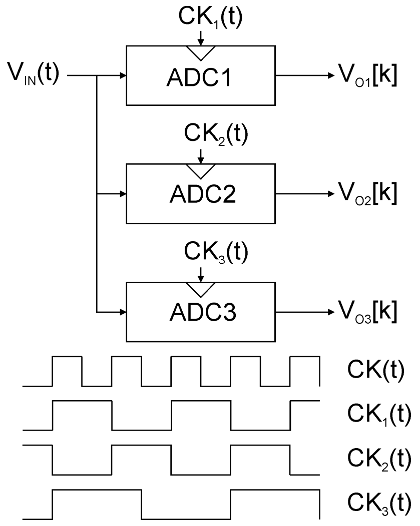

Figure 1. Architecture of the TI-ADC with reference channel.

outputs of the different channels. However mismatches among the channels reduce the linearity achievable by using time-interleaving technique [3], thus calibration is required.
Calibration using a LMS algorithm requires a model of the system to be calibrated: the i-th channel of the TI-ADC can be modeled with an offset ε_{Oi}, a gain error ε_{Gi} and a timing error ε_{Ti}:

$$V_{Oi}[k] = \varepsilon_{Oi} + \left(1+\varepsilon_{Gi}\right) V_{IN}\left(kT_S - \varepsilon_{Ti}\right) \quad (1)$$

where V_{Oi} is the analog equivalent of the output code, and here and in the following we neglect the quantization error. Timing errors make the output a function not of the input samples, but of the input analog waveform; however by a first order Taylor expansion the output can be expressed as a function of the samples of the input and of its time derivative: $V_{IN}\left(kT_S - \varepsilon_{Ti}\right) \approx V_{IN}[k] - \varepsilon_{Ti} V'_{IN}[k]$, where $V'_{IN}[k] = \left(dV_{IN}/dt\right)_{t=kT_S}$. Since only the mismatch between the two channels is relevant to nonlinear errors, it is possible to redefine each error source as $\varepsilon_{X1}=\varepsilon_X$ and $\varepsilon_{X2}=\varepsilon_X+\delta_X$ (X=O, G or T), so that the output of the converter can be expressed as:

$$V_{OUT}[k] \cong V_{IN}[k] + \varepsilon_O + \varepsilon_G V_{IN}[k] - \varepsilon_T V'_{IN}[k] + \delta_O R_E[k] + \delta_G R_E[k] V_{IN}[k] - \delta_T R_E[k] V'_{IN}[k]. \quad (2)$$

where R_E is a sequence that is equal to one for the even samples (converted by ADC2) and zero for the odd ones.
Knowledge of δ_O, δ_G and δ_T suffices to correct for nonlinear errors, thus maximizing linearity, although the calibrated output will be affected by an offset, a gain error, and a linear delay.
In order to calibrate for mismatches between the two channels without interrupting ADC operation, it is necessary to introduce an auxiliary channel to be used as reference ADC. The additional ADC generates the reference signal for the LMS algorithm, to minimize the error energy and thus maximize the linearity of the converter. The reference ADC allows an indirect comparison between the two channels, that operate on different samples of the input signal: this requires that the clock frequency for the reference channel is chosen so that it alternately converts an odd and an even sample of the input signal. Fig. 1 shows the architecture of the TI-ADC, that is composed of two ADCs at half sampling frequency (ADC1 and ADC2, clocked at $f_S/2$), that convert the odd and even samples respectively, and a third reference ADC (ADC3) clocked at $f_S/3$, so that its first sample is the same as that of ADC1 (sample 1), its second is the same as the second of ADC2 (sample 4), and so on.
Two least mean squares (LMS) loops operating alternately and using one input sample every six are used to correct the ADC channels against the reference channel. The model developed so far allows obtaining the error function that has to be minimized by the LMS algorithm to estimate the error parameters and thus correct the errors of the TI-ADC in the digital domain. In particular, we have to calculate for both constituent channels (i=1, 2) the mismatch coefficients δ_{Oi}, δ_{Gi}, δ_{Ti}, as defined in (2), with respect to the reference channel (i=3). We are assuming $\varepsilon_{X3}=\varepsilon_X$, $\varepsilon_{Xi}=\varepsilon_X+\delta_{Xi}$ (X=O, G, T, and i=1, 2).
Let's consider the first LMS loop (the other, which calibrates the second ADC, is identical) to illustrate the calibration algorithm. The outputs of the first and third ADCs are, respectively:

$$V_{O1}[k] \simeq \varepsilon_{O1} + \left(1+\varepsilon_{G1}\right) V_{IN}[k] - \varepsilon_{T1} V'_{IN}[k] \qquad V_{O3}[k] \simeq \varepsilon_{O3} + \left(1+\varepsilon_{G3}\right) V_{IN}[k] - \varepsilon_{T3} V'_{IN}[k]. \quad (3)$$

The difference between the two expressions should be zero, neglecting quantization error and noise, if no non-ideal effects are present. The error function to be minimized is therefore:

$$V_{O1}[k]-V_{O3}[k]\simeq\delta_{O1}+\delta_{G1}V_{IN}[k]-\delta_{T1}V'_{IN}[k]+\theta \tag{4}$$

where θ takes into account noise, quantization error, stochastic jitter and unmodeled errors in the converters. Eq. (4) requires an approximate estimation of the input and of its first derivative: the former can be easily provided by the non-corrected output of the ADC $\tilde{V}_{IN}[k]=V_{OUT}[k]=V_{Oi}[k]$, whereas the derivative of the input signal can be approximated by that of the output

$$\tilde{V}'_{IN}[k]=V'_{OUT}[k]\triangleq V_{OUT}[k]\otimes h_D[k] \tag{5}$$

where $h_D[k]$ is the impulse response of the differentiator filter and the symbol ⊗ means convolution. It has to be noted that the computation of $V'_{OUT}[k]$ requires both the samples of the first and of the second channel, and it is affected by the errors of both. This is a second order problem, however, because the least squares algorithm which is used to estimate the error parameters minimizes the difference between the outputs of the calibrated and the reference ADCs, which is all that is required to minimize the nonlinearity of the overall converter.
In the more general case of a M-channel TI-ADC, a reference channel working at a sampling frequency of f_S/N, with N co-prime with M, has to be used. There must be M LMS loops to calibrate each of the M ADCs with the reference channel, that are updated every M*N samples, when the i-th ADC and the reference ADC are aligned.

III. Nyquist differentiator filters

The previous Section has shown the need to compute the derivative of the input signal to estimate the timing error. The ideal differentiator filter, however, cannot be implemented, and approximations are required to have realizable filters. These approximations may introduce phase and amplitude errors, thus limiting their application to signals spanning a more or less limited fraction of the Nyquist band. The linear (amplitude and phase) errors introduced by the differentiator filter will affect both the timing error estimation algorithm and the subsequent digital correction of the error terms. The larger the usable bandwidth of the (realizable) differentiator filter, the better the calibration algorithm will perform with wideband input signals.
The most straightforward way to implement a differentiator filter is by exploiting the inverse Discrete-Time Fourier Transform (DTFT) of $H(e^{j\omega})=j\omega$ ($-\pi<\omega<\pi$). It is possible to obtain a causal FIR filter by truncating the impulse response and shifting it to the right; windowing must be employed to avoid the Gibbs phenomenon.
An alternative approach is to use two fractional delay filters, to obtain a differentiator such as the one depicted in Fig. 2. The derivative, in fact, can be approximated as:

$$V'[k]\approx\left[V(kT_S+\Delta)-V(kT_S-\Delta)\right]/2\Delta \tag{5}$$

for small values of Δ. A commonly used fractional delay filter is the Thiran filter [7], which is an all-pass IIR filter whose coefficients depend on the filter order N and the fractional delay Δ > N-1 (this last condition is required for stability). The filter transfer function is:

$$H(z)=\frac{z^{-N}A(z^{-1})}{A(z)}=\frac{a_N+a_{N-1}z^{-1}+...+a_0z^{-N}}{a_0+a_1z^{-1}+...+a_Nz^{-N}} \qquad a_k=\begin{cases}(-1)^k\binom{N}{k}\prod_{i=0}^{N}\frac{\Delta-N+i}{\Delta-N+k+i} & k=1,2,...N\\ 1 & k=0\end{cases} \tag{6}$$

In [8] it is shown that the differentiator based on Thiran fractional-delay filters degenerates into a FIR filter for $\Delta\to 0$, so that the stability problems inherent in IIR filters are not a concern.

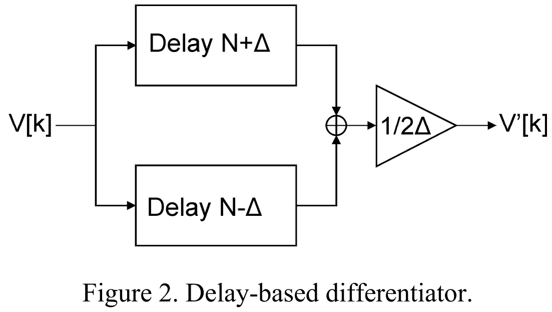

Figure 2. Delay-based differentiator.

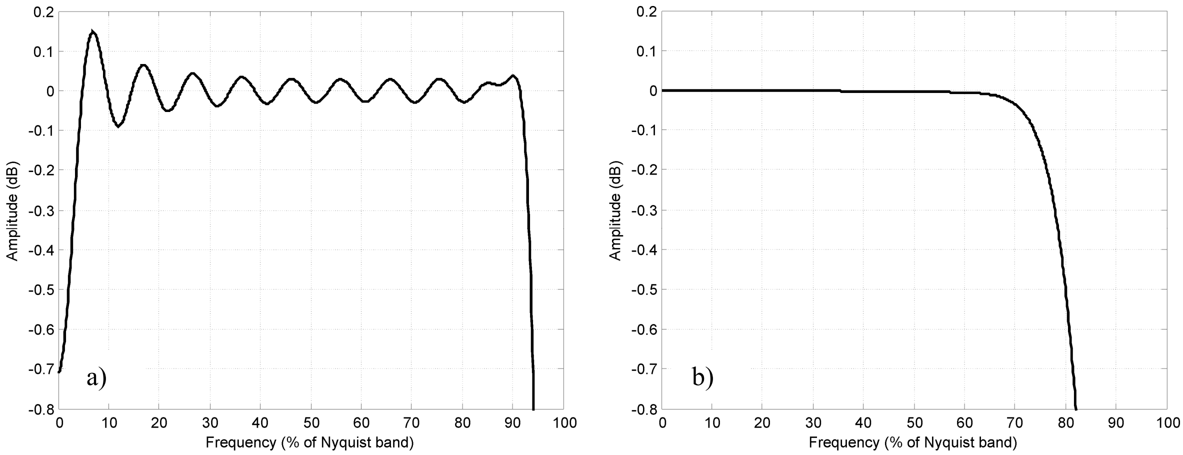

Figure 3. Amplitude error (a) of the standard FIR differentiator (N=41, Hamming window) and (b) of the Thiran-based FIR differentiator (N=41).

Fig. 3 shows the amplitude errors of 41^{th} order FIR differentiators based on the DTFT and on Thiran respectively. The Thiran-based filter works best from dc to about 75% of the Nyquist band, while the Hamming windowed FIR filter works best at higher frequencies, but has higher errors at low frequency and its in-band average error is higher. Phase errors are zero at all frequencies by construction in both the standard and the Thiran-based differentiator.

IV. Differentiating undersampled signals

If the input signal lies beyond the Nyquist frequency, it will be undersampled by the sampling process, and this implies a frequency translation to baseband, as shown in Fig. 4 for even-order and odd-order undersampling. Additionally, a flip in the frequency spectrum is present in the even-order case. As a consequence, the derivative of the output baseband signal is not a sampled version of the derivative of the input, therefore a more complicated filtering block than what was used in the previous Section is needed to estimate it.
The use of the low-frequency analogical components of the signal can be useful to derive such a differentiator filter. Given a signal with spectrum V(f), we can decompose it in two complex signals containing only the right-half plane (RHP) spectrum $V_P(f)$ and the left-half plane (LHP) spectrum $V_L(f)$, that can be calculated by exploiting the Hilbert transform $V_H(f)=-j\mathrm{sgn}(f)V(f)$:

$$2V_P(f)=V(f)+jV_H(f) \qquad 2V_N(f)=V(f)-jV_H(f) \qquad V(f)=V_P(f)+V_N(f). \qquad (7)$$

This decomposition can be applied to the undersampled signal, and this enables to express the original signal as a translation of the RHP and LHP spectra of the undersampled signal toward the right and left, respectively.
Let's consider by example the situation in Fig. 4b, where the input signal V_3 is in the third Nyquist band. The undersampled (output) signal $V_1(t)$ and the original signal in the third Nyquist band $V_3(t)$ occupy different bands but have the same values at the sampling instants kT_S. By applying (7) we obtain:

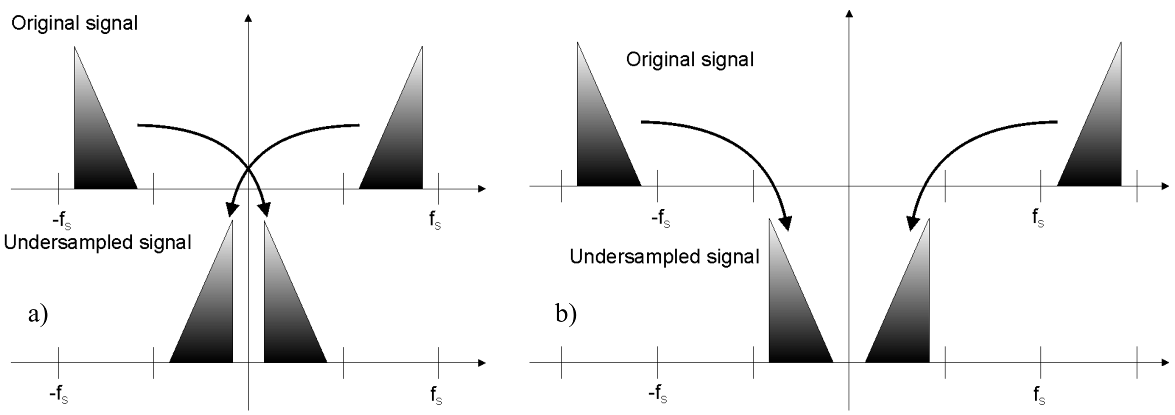

Figure 4. Even-order (a) and odd-order (b) undersampling.

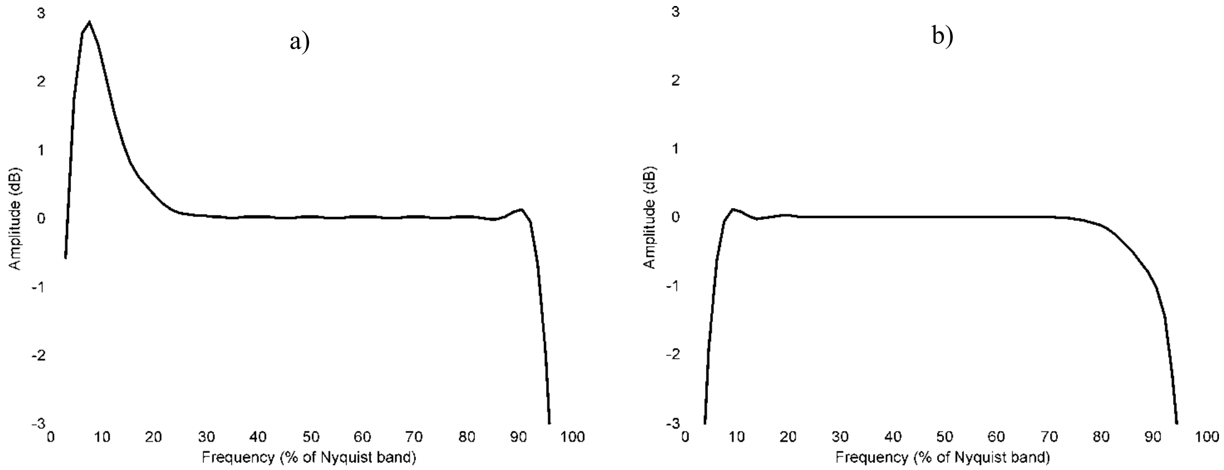

Figure 5. Amplitude error of the differentiator for the second (a) and third (b) Nyquist bands.

$$V_{3P}(f)=V_{1P}(f-f_S) \qquad V_{3N}(f)=V_{1N}(f+f_S) \tag{8}$$

thus exploiting the modulation theorem we can express the original signal as:

$$V_3(t)=\left[V_1(t)+jV_{1H}(t)\right]e^{2\pi f_S t}+\left[V_1(t)-jV_{1H}(t)\right]e^{-2\pi f_S t}=V_1(t)\cos(2\pi f_S t)-V_{1H}(t)\sin(2\pi f_S t). \tag{9}$$

This signal can be differentiated and sampled, obtaining the relationship between the first derivative of the original signal and the undersampled signal (and its derivative), that shows that computation of the trigonometric functions is not required:

$$V_3'[k]=\left[V_1'[k]-2\pi f_S V_{1H}[k]\right]\cos(2\pi k)-\left[V_1'[k]+2\pi f_S V_{1H}[k]\right]\sin(2\pi k)=V_1'[k]-2\pi f_S V_{1H}[k]. \tag{10}$$

Eq. (10) shows that the required filter can be implemented by a discrete Hilbert filter, made causal and realizable by shifting and windowing, and a differentiator filter. This result can be generalized to different Nyquist bands, by changing amplitude and sign of the coefficient that multiplies the Hilbert transform. The general formulae to compute the first-order derivative of a signal in the 2m and in the 2m+1 Nyquist bands are respectively:

$$V_{2m}'[k]=V_1'[k]+2m\pi f_S V_{1H}[k] \qquad V_{2m+1}'[k]=V_1'[k]-2m\pi f_S V_{1H}[k]. \tag{11}$$

Fig. 5 shows the amplitude error of the filters for the second and third Nyquist bands respectively, highlighting a wideband behavior. Both differentiators use 41-tap Thiran-based FIR filters and 41-tap Hilbert filters using Blackman windowing. Signals spanning from 20% to 80% of the Nyquist band can be accurately differentiated.

V. Simulation results

To verify the proposed calibration procedure, we have performed extensive simulations in Matlab on a two-channel 14-bit TI-ADC. Each constituent ADC, including the reference channel, has been modeled with offset, gain and timing errors, described as Gaussian variables with zero mean and a variance of 0.2 % (1% for timing errors). Error parameters are different for the different channels, thus introducing random mismatches. The differentiator filters used in the calibration algorithm are 41-tap FIR filters based on the Thiran architecture; for undersampled signals, Hilbert filters with 41-tap Blackman windows have also been used.
Fig. 6 shows the behavior of the algorithm for an input signal in the second and third Nyquist band, respectively, and Tab. I reports the statistical characterization of total harmonic distortion (THD) and spurious free dynamic

Table I: Simulation results for multi-tone signals in different Nyquist bands.

	PRE-CALIBRATION				POST-CALIBRATION			
	SFDR (dB)		THD (dB)		SFDR (dB)		THD (dB)	
BAND	MEAN	STD	MEAN	STD	MEAN	STD	MEAN	STD
I	37.6	8.3	-41.0	5.4	84.5	3.2	-70.3	4.3
II	36.1	6.8	-34.2	7.0	81.0	4.7	-66.5	5.6
III	37.5	9.2	-30.7	7.8	79.3	5.9	-64.6	7.0

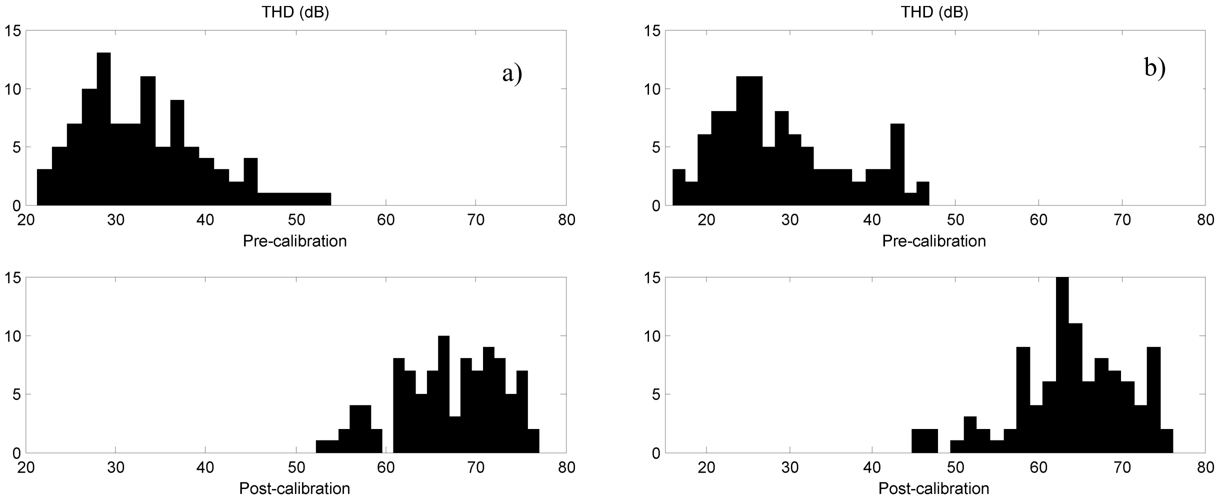

Figure 6. Histograms of THD for a multi-tone input in the second (a) and third (b) Nyquist band.

range (SFDR) before and after calibration, for the first three Nyquist bands. A multi-tone input signal spanning about the 50% of the Nyquist band around its center has been considered, and a linearity improvement of more than 32 dB (5 bits) is achieved.

VI. Conclusions

This paper presents a digital background calibration technique for time-interleaved analog-to-digital converters, that builds on literature results to improve signal bandwidth limitations with minimal hardware overhead.
The proposed calibration algorithm allows signals spanning a wide fraction of the Nyquist bandwidth, thanks to a suitable choice of the differentiator filter needed for timing skews estimation and correction. Moreover, wideband differentiator filters suitable for undersampled signals are proposed, thus allowing calibration also in case of signals beyond the first Nyquist band. Simulations show the feasibility of the technique for the second and the third Nyquist band, but in principle it can be extended to higher order Nyquist bands.
The algorithm can be easily extended to TI-ADCs with more than two channels, by using more LMS calibration loops and with a suitable choice of the clock frequency for the reference channel. The overhead of the technique in terms of area and power consumption is mainly due to the need for this reference channel, and this overhead is reduced when the number of channels is increased. For a M-channel TI-ADC the main cost is in terms of calibration speed because parameter updates for a given channel occur once every N samples.

References

[1] S. M. Louwsma, A. J. M. Van Tuijl, M. Vertregt, B. Nauta, 'A 1.35 GS/s, 10 b, 175 mW time-interleaved AD converter in 0.13 μm CMOS,' *IEEE J. Solid-State Circuits*, vol. 43, no. 4, pp. 778-786, Apr. 2008.
[2] S.-W. Sin, S.-P- U, R. P. Martins, '1.2-V, 10-bit, 60-360 MS/s time-interleaved pipelined analog-to-digital converter in 0.18 μm CMOS with minimised supply headroom,' *IET Circuits, Devices & Systems*, vol. 4, no. 1, pp. 1-13, Jan. 2010.
[3] M. Gustavsson, J. J. Wikner, N. Tan, *CMOS data converters for communications*, Kluwer Academic Publ.: New York, 2002.
[4] J. A. McNeill, C. David, M. Coln, R. Croughwell, '"Split ADC" calibration for all-digital correction of time-interleaved ADC errors,' *IEEE Trans. Circuits and Systems Part II*, vol. 56, no. 5, pp. 344-348, May 2009.
[5] T. Oshima, T. Takahashi, T. Yamawaki, 'LMS calibration of sampling timing for time-interleaved A/D converters,' *IET Electron. Lett.*, vol. 45, no. 12, pp. 615-617, Jun. 2009.
[6] S. M. Jamal, D. Fu, M. P. Singh, P. J. Hurst, S. H. Lewis, 'Calibration of sample-time error in a two-channel time-interleaved analog-to-digital converter,' *IEEE Trans. Circuits and Systems Part I*, vol. 51, no. 1, pp. 130-139, Jan. 2004.
[7] T. I. Laakso, V. Valimaki, M. Karjalainen, U. K. Laine, 'Splitting the unit delay,' *IEEE Signal Processing Mag.*, vol. 13, no. 1, pp. 30-60, Jan. 1996.
[8] C.-C. Tseng, 'Digital differentiator design using fractional delay filter and limit computation,' *IEEE Trans. Circuits and Systems Part I*, vol. 52 , no. 10, pp. 2248-2259, Oct. 2005.